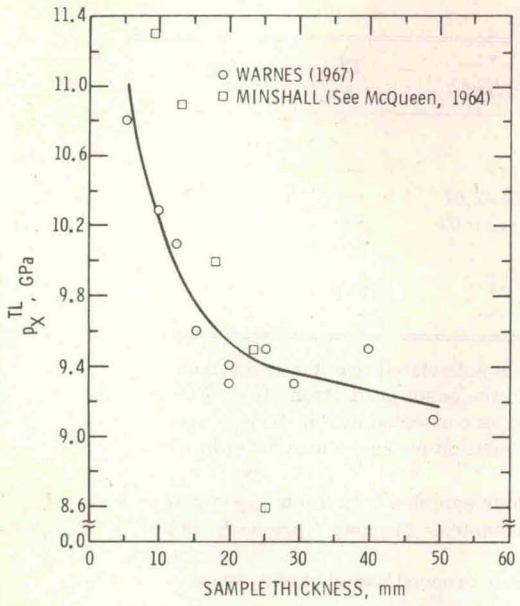

FIG. 24. The transition stress for antimony observed under shock loading has been found to exhibit an unusually slow transformation rate. The slow rate is manifested as a strong dependence of the observed transition stress on sample thickness.

is consistent with the static observations.

Thickness variations of p_x^{TL} observed by Warnes for thicknesses less than 20 mm are well fitted by a relaxation time $t_0 = 3$ μs in Eq. (55). This relaxation time is at least an order of magnitude larger than that for thin samples of iron (Forbes, 1976). A single transformation rate cannot explain the behavior indicated by measurements at thicknesses less than and greater than 20 mm.

Further evidence for nonequilibrium thermodynamic behavior in the shock-induced transition is contained in the data of Warnes in the mixed phase region about 8.8 GPa, where the Hugoniot curve is observed to lie above the equilibrium curve.

A flash x-ray profile of shocks in antimony in two-dimensional steady flow was later reported by Breed and Venable (1968). Figure 2 of their paper was an overlay of a flash radiograph of a wave pattern in two-dimensional flow produced by detonation of the high explosive, baratol, in contact with antimony. The figure showed profiles of a Plastic I wave associated with the phase transition and a Plastic II wave corresponding to the input pressure produced in antimony. They directed particular attention to the curvature of the Plastic II wave front, which indicates that the wave starts at a very low velocity and accelerates rather rapidly to its final velocity, which differs but slightly from the velocity of the Plastic I wave.

This curvature is a rational consequence of the finite transition rate and Plastic I decay noted by Warnes. From the jump conditions, Eqs. (9) and (10), with U_1, V_0, P_0, P, V replaced by $U_{p1}, V_1, P_1, P_2, V_2$, respectively, velocity of the second shock is

$$U_{s2} = U_{p1} + V_1[(P_2 - P_1)/(V_1 - V_2)]^{1/2}.$$

With P_2 and V_2 fixed and P_1 and ρ_1 decreasing, the second shock accelerates. With a relatively simple transformation this result can be applied to the Breed and Venable radiograph. The Plastic II profile so calculated is shown as OB in Fig. 25. Measurements by Breed and Venable (1968) are indicated by curve OB'. The calculated profile reproduces essential features of the observation, though differences remain (Duvall, 1973).

Hayes (1972), using a formalism slightly different from that in Sec. II.F, has inferred from the thin-sample data of Fig. 24 a transformation time of 2.3 μs. This time is in reasonable agreement with the observed value of 2–3 μs for the time delay of formation of the Plastic II wave reported by Breed and Venable (1968). Forbes (1976) shows relations among the various formalisms which have been used.

E. Bismuth

The temperature–pressure phase diagram of bismuth has been the subject of much study, which will undoubtedly continue. Its many polymorphic transitions are especially important because of their use as fixed-point calibrations. The Bi I→ Bi II and melting transitions are of particular interest under shock loading since they afford an excellent opportunity to develop our understanding of transitions based on carefully characterized static high-pressure studies. A recent summary of the Bi phase diagram is given by Liu *et al.* (1973).

The investigation of bismuth under shock loading by Duff and Minshall (1957) is one of the classic papers of shock-wave physics. Measurements of the solid I → solid II and the solid I→ liquid transitions were attempted. The solid I→ solid II transition was apparently detected, but pressure of the transition was about 250 MPa higher than would be expected from static measurements. Transformation rates were apparently very rapid since values for p_x^{TL} were found to be independent of sample thickness. In experiments at elevated temperature, Duff and Minshall failed to observe evidence for melting in the wave profiles, even though pressure and temperature were in the equilibrium liquid region as determined by static pressure measurements. Because of the importance of these transitions, the disagreement between static and shock loading results raised serious questions about the nature of shock-induced transitions. Further experiments by Hughes *et al.* (1961) under shock loading were inconclusive in resolv-

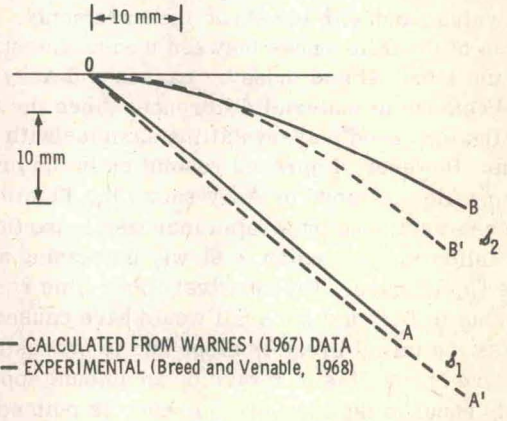

FIG. 25. Observed and calculated Plastic I and Plastic II wave fronts in antimony in two-dimensional steady flow.

TABLE III. Bi I→ Bi II transition[a] (normalized to 295 K).

Author	p_x^{TL} GPa	$\bar{p}^{TL}$ GPa	P^T GPa	η_{TL} %
Shock loading				
Duff and Minshall, 1957[b]	2.69–2.75	···	···	6.5–6.7
Larson, 1967[c]	2.46–2.56	2.43–2.57	···	5.8–6.1
Asay, 1974[d]	2.50–2.53	2.55±0.03	···	5.8
Static loading				
Heydemann, 1967a, 1967b	···	···	2.55	···
Giardini and Samara, 1965	···	···	···	6.4

[a] p_x^{TL} is the stress observed under shock loading which is associated with the transition; η_{TL} is the volume compression from atmospheric pressure to the onset of the transition; $\bar{p}^{TL}$ is the mean pressure calculated from p_x^{TL}. The value shown is corrected by +90 MPa to account for a 20 K shock-induced temperature rise. P^T is the transition pressure measured in a hydrostatic environment.

[b] The range shown corresponds to values observed on four samples with 3 mm grain size.

[c] The range shown corresponds to values observed on samples: 21 cast, 7 pressed, and 7 single-crystal.

[d] The range shown corresponds to values observed in four pressed samples with 30μm grain size.

ing the questions raised by the work of Duff and Minshall.

Larson (1967) investigated the solid I→ solid II transition under shock loading, using wave profile measurements made with the quartz gauge. Thirty-five different samples were shocked, including cast and pressed polycrystalline and single-crystal samples. With his improved time resolution, compared with that available to Duff and Minshall, Larson measured the HEL and showed that the transition wave has considerable structure. When a correction is made for shear strength and for a +90 MPa difference in pressure due to a 20 K shock-induced temperature rise, his data are found to be in excellent agreement with the static pressure determination. Larson's and other shock measurements are shown in Table III and compared with static data.

Asay (1974) used projectile impact loading and detected wave profiles with the VISAR to study both the solid I→ solid II and solid I→ liquid transition. (His melting transition measurements are described in Sec. VI.B.) Since the VISAR is insensitive to wave front tilt, even better wave profile resolution was obtained than that reported by Larson. As shown in Table III, Asay's measurements of p_x^{TL} are in good agreement with Larson's values and with the static measurements.

Some of the differences between measurements by Duff and Minshall and those by Larson and Asay may have been due to material differences since the former investigators used polycrystalline samples with large grains. However, improved resolution in the pressure–time profiles obtained by Asay shows the Plastic I wave to be characterized by a rapid increase in particle velocity followed by a region of slowly increasing amplitude in the (p_x, t) plane. The relatively poor time resolution available to Duff and Minshall would have caused them to miss the initial break in slope and to overestimate the pressure of the Plastic I wave by an amount approximately equal to their reported error, as pointed out by Asay. This illustrates a point that must always be kept in mind when assessing numerical results of shock wave experiments: there is frequently an arbitrary element in the interpretation of experimental records which may result from instrumental deficiencies or may reflect attempts to oversimplify the records. This arbitrariness produces, in turn, some uncertainty in the numerical results. There are exceptional situations where interpretation is unambiguous, but, in general, the significance of agreement between static and shock loading results should be assessed with careful analysis of the characteristics of the instrumentation and the uncertainty associated with kinetic and shear strength effects.

By shock loading into the melt region, Asay determined the pressure of the solid I–solid II–liquid triple point. His pressure determination, which is the mean of nine different measurements, is shown in Table IV. Again, there is good agreement between static and shock loading results.

The lower-pressure phase diagram shown in Fig. 26 indicates that shock and static loading data at various temperatures are in good agreement. Thus, the more modern wave profile measurements show that static and shock loading measurements in bismuth are in good agreement. It does not appear that more accurate determinations will be achieved in bismuth under shock

TABLE IV. Triple point determinations Bi I→ liquid→ Bi II.

Author	p_x^{TL} GPa	Temperature K
Shock loading		
Asay, 1974	$1.70^{+0.08}_{-0.05}$[a]	···
Static loading		
Bridgman, 1935	1.70	456
Bundy, 1958	1.52	453
Panova *et al.*, 1961	1.72	457
Klement *et al.*, 1963	1.67	464

[a] ± indicates range of values determined for different samples and under different initial temperatures. No attempt has been made to apply a strength correction.